Cell. Mol. Life Sci. (2011) 68:3275–3292
DOI 10.1007/s00018-011-0639-0

Cellular and Molecular Life Sciences

RESEARCH ARTICLE

The sheddase activity of ADAM17/TACE is regulated by the tetraspanin CD9

Maria Dolores Gutiérrez-López · Alvaro Gilsanz · María Yáñez-Mó · Susana Ovalle · Esther M. Lafuente · Carmen Domínguez · Peter N. Monk · Isidoro González-Alvaro · Francisco Sánchez-Madrid · Carlos Cabañas

Received: 30 September 2010 / Revised: 23 December 2010 / Accepted: 20 January 2011 / Published online: 2 March 2011

Abstract ADAM17/TACE is a metalloproteinase responsible for the shedding of the proinflammatory cytokine TNF-α and many other cell surface proteins involved in development, cell adhesion, migration, differentiation, and proliferation. Despite the important biological function of ADAM17, the mechanisms of regulation of its metalloproteinase activity remain largely unknown. We report here that the tetraspanin CD9 and ADAM17 partially co-localize on the surface of endothelial and monocytic cells. In situ proximity ligation, co-immunoprecipitation, crosslinking, and pull-down experiments collectively demonstrate a direct association between these molecules. Functional studies reveal that treatment with CD9-specific antibodies or neoexpression of CD9 exert negative regulatory effects on ADAM17 sheddase activity. Conversely, CD9 silencing increased the activity of ADAM17 against its substrates TNF-α and ICAM-1. Taken together, our results show that CD9 associates with ADAM17 and, through this interaction, negatively regulates the sheddase activity of ADAM17.

Keywords Tetraspanins · CD9 · ADAM17 · TACE · TNF-α · ICAM-1

Abbreviations

BSA	Bovine serum albumin
DTSSP	3,3′-Dithiobis-sulfosuccinimidylpropionate
EGFR	Epidermal growth factor receptor
FCS	Fetal calf serum
FITC	Fluorescein isothiocyanate
HMEC-1	Human microvasculature endothelial cells-1
HRP	Horse radish peroxidase

M. D. Gutiérrez-López, A. Gilsanz and M. Yáñez-Mó contributed equally to this work.

Electronic supplementary material The online version of this article (doi:10.1007/s00018-011-0639-0) contains supplementary material, which is available to authorized users.

M. D. Gutiérrez-López · A. Gilsanz · S. Ovalle · C. Cabañas (✉)
Centro de Biología Molecular Severo Ochoa (CSIC-UAM), Nicolás Cabrera 1, Campus de Cantoblanco, 28049 Madrid, Spain
e-mail: ccabanas@cbm.uam.es

M. Yáñez-Mó · F. Sánchez-Madrid
Servicio de Inmunología, Hospital Universitario de La Princesa, Instituto de Investigacion Sanitaria Princesa, 28006 Madrid, Spain

F. Sánchez-Madrid
Departamento de Biología Vascular e Inflamación, CNIC, 28029 Madrid, Spain

E. M. Lafuente · C. Cabañas
Departamento de Microbiología I (Inmunología), Facultad de Medicina, UCM, 28040 Madrid, Spain

C. Domínguez · I. González-Alvaro
Servicio de Reumatología, Hospital Universitario de La Princesa, 28006 Madrid, Spain

P. N. Monk
University of Sheffield Medical School, Sheffield S10 2RX, Sheffield, United Kingdom

Present Address:
M. D. Gutiérrez-López
Departamento de Farmacología, Facultad de Medicina, Universidad Complutense, 28040 Madrid, Spain

HUVECs	Human umbilical vein endothelial cells
PBLs	Peripheral blood lymphocytes
PBS	Phosphate buffered saline
PMA	Phorbol myristate acetate
mAb	Monoclonal antibody
TACE	Tumor necrosis factor alpha converting enzyme
TBS	Tris buffered saline
TEMs	Tetraspanin-enriched microdomains
TNF-α	Tumor necrosis factor-α
SDS-PAGE	Sodium dodecyl sulfate polyacrylamide gel electrophoresis

Introduction

ADAM17 (also termed TACE: TNF-alpha converting enzyme) was identified as the enzyme cleaving TNF-α from its transmembrane precursor form, and later found to cleave also the ectodomains of other cell surface proteins that are critically involved in development, cell growth, adhesion, differentiation and migration of leukocytes and tumor cells (see for review [1–3]). ICAM-1 and VCAM-1, two crucial endothelial molecules mediating leukocyte extravasation, are also shed by ADAM17 [4, 5] and elevated soluble levels of these proteins have been found in several inflammatory and tumoral pathologies [6]. The importance of ADAM17 is demonstrated by the perinatal lethality observed in knockout mice, due to defective cardiac valvulogenesis [7]. The physiological and pathological relevance of ADAM17 substrates suggests that its proteolytic activity must be finely regulated. The mechanisms controlling ADAM17 activity remain largely unknown; several possibilities have been proposed, including regulation through phosphorylation of its cytoplasmic tail, interaction with regulatory proteins involved in cell signaling or accessibility to substrates [2, 8].

CD9 was initially identified as a lymphohematopoietic marker and later implicated in diverse functions, including cell signaling, growth, adhesion, motility, tumorigenesis, metastasis, and sperm-egg fusion [9–12]. Like other tetraspanins, CD9 participates in the organization of a type of cell surface microdomains—the tetraspanin web— through lateral association with additional tetraspanins and transmembrane proteins [13–15]. CD9 forms complexes with several β1 integrins, influencing integrin-mediated phenomena such as adhesion, migration, signaling, and proliferation in different cell systems [12, 16]. CD9 also regulates bombesin-stimulated ADAM10-dependent cleavage of HB-EGF [8, 17] and the interaction of sperm ADAM2 and ADAM3 with egg integrin α6β1 [11, 18]. Interestingly, regulation of the constitutive ADAM10-mediated cleavage of EGF and TNF-α by antibodies directed to different tetraspanins, including CD9, has been recently reported [19].

We report here that CD9 interacts with ADAM17 on the surface of leukocytes and endothelial cells; through these interactions CD9 exerts negative regulatory effects on ADAM17-mediated shedding of TNF-α and ICAM-1.

Materials and methods

Cells and antibodies

The human endothelial HMEC-1 cell line was grown in MCDB-131 medium supplemented with 20% FCS, 10 ng/ml recombinant human EGF (Promega, Madison WI), and 1 μg/ml hydrocortisone (Sigma) on gelatin-coated flasks. HUVECs were obtained and cultured as described [20]. The human EA-hy926 endothelial cell line (generous gift from Dr. C. J. Edgell) was grown in DMEM)–was grown in DMEM–10% FCS medium. The human monocytic THP-1 and T leukemic Jurkat cell lines were from the ATCC. PBLs were isolated from healthy donors by Histopaque-1077 density-gradient centrifugation (Sigma Diagnostics) and removal of monocytes by adhesion to plastic dishes, as described [21]. HUT78 T lymphocytes, Colo320 colon carcinoma, and CD9-stably transfected Colo320 cells [22] were cultured in RPMI 1640-10% FCS. Raji/vector and Raji/CD9 cells stable transfectants were obtained by electroporating human Raji B cells at 2.5 kV/cm using an ElectroSquarePorator ECM 830 (BTX) with empty pcDNA3 vector (Invitrogen) or vector containing CD9 cDNA. After transfection, cells were selected with medium containing 0.9 mg/ml G418.

Anti-β1 integrin (TS2/16), anti-CD9 (VJ1/20, VJ1/10, PAINS-13), anti-CD147 (VJ1/9) and anti-CD151 (Lia 1/1) mAbs have been previously described [22–24]. mAb anti-ICAM-1 Hu5/3 was kindly provided by FW Luscinskas, (Brigham and Women's Hospital, Boston, USA). Anti-CD59 (PAINS-19), anti-HASP8 (PAINS-18), anti-CD81 (5A6) and anti-CD82 (TS82) were also used as controls. Rabbit polyclonal anti-human CD151 antibody H-80 was purchased from Santa Cruz Biotechnology. Anti-human ADAM17/TACE Abs used were: mAb 5C2 and 2A10 (obtained in our laboratory); mAb clones 111633 and 111623 from R&D Systems; rabbit polyclonal H-170 and H-300 Abs from Santa Cruz Biotechnology. Anti-TNF-α Ab Infliximab (Remicade®, Schering Plough) was biotinylated as previously described [12]. Anti-GST goat polyclonal Ab was from Amersham Biosciences (Uppsala, Sweden).

Flow cytometry, immunofluorescence, and confocal microscopy

Surface expression of proteins was analyzed by flow cytometry as previously described [22]. For immunofluorescence experiments, cells were grown on 12-mm glass coverslips (precoated with 1% gelatin for HMEC-1 cells) and fixed with 4% formaldehyde in PBS. For double-staining, fixed cells were incubated with the appropriate primary antibody followed by Alexa Fluor™ 488 goat anti-mouse IgG conjugate (Invitrogen, Barcelona, Spain). After incubation with mouse serum, cells were incubated with the appropriate biotinylated mAb followed by rhodamine Red-X-streptavidin (Invitrogen). Cells were mounted with Mowiol (Calbiochem). Optical sections were obtained with a Leica TCS-SP5 confocal laser scanning unit attached to a Leica DMIRBE inverted epifluorescence microscope (Leica Microsystems, Heidelberg, Germany).

In situ proximity ligation assays (PLAs)

Duolink IQ PLAs is a validated technology (Olink Bioscience, Uppsala, Sweden) that allows detection of protein–protein interactions in cell samples prepared for microscopy. Cells were incubated with anti-ADAM17 mAb (clone 111633 from R&D Systems), anti-CD147 mAb VJ1/9 or anti-CD81 mAb 5A6 on the one hand, followed by specific oligonucleotide-labeled secondary antibody (anti-mouse-plus probe), followed by biotinylated anti-CD9 mAb VJ1/20, and anti-biotin-minus probe after blocking with non-immune mouse serum. Only if the two different target molecules are in close proximity (in the range of 50 nm), the oligonucleotides of the two probes will hybridize and after a rolling-circle amplification reaction and detection with a different fluorescently labeled oligonucleotide a fluorescent dot signal can be visualized and analyzed by microscopy.

Protein cross-linking and co-immunoprecipitation

HMEC-1 or THP-1 cells (untreated or treated with 20 ng/ml of PMA) were lysed for 30 min at 4°C in TBS-1% Brij-97 containing 1 mM $CaCl_2$ and 1 mM $MgCl_2$ and protease inhibitors. Cell lysates were microcentrifuged 15 min at 13,000 rpm. Specific antibodies were bound to Protein A-Sepharose for 2 h at 4°C and then incubated with lysates overnight at 4°C. Beads were then washed three times with 1:10 diluted lysis buffer and immune complexes boiled in Laemmli buffer, resolved by SDS-PAGE, and transferred to nitrocellulose membranes. Blots were blocked with TBS + 5%BSA and developed with the corresponding primary antibody followed by incubation with secondary peroxidase-coupled antibodies (Sigma). Chemiluminescence was detected with ECL detection kit (Amersham Biosciences). Total protein concentration in whole cellular lysates was calculated using the DC protein assay (Bio-Rad Laboratories). Where indicated, bands were quantified using a Bio-Rad GS-800 densitometer and analyzed with the Quantity One Software.

In cross-linking experiments, cells were incubated for 30 min with the membrane impermeable and thiol-cleavable cross-linker DTSSP (Pierce-Thermo Scientific, Rockford, IL) at 1 mM in PBS, followed by blockade in TBS, cell lysis in 1% Triton-X100, immunoprecipitation with respective antibodies and SDS-PAGE under reduced conditions to cleave the thiol bonds within the cell surface cross-linked proteins. Presence of ADAM17 after reduction of cross-linked complexes was identified by immunoblotting with the H-300 Ab, which detects unprocessed and mature ADAM17 under reducing conditions. Assessment of effective immunoprecipitation with the different Abs was carried out in parallel gels under non-reducing conditions.

Protein–protein interaction assays

The human wtCD9-LEL-GST and wtCD81-LEL-GST fusion proteins as well as CD9-LEL-GST mutants with Cys152, Cys153, Cys167 or Cys181 replaced by alanines, were produced and purified as described [20, 25]. The cDNA encoding the full-length extracellular domain of ADAM17 linked to the human IgG constant region (ADAM17-Fc) was kindly provided by Dr. M. Humphries and purified from supernatants of transiently transfected COS-1 cells as described [26]**.** The GST-PAK-CRIB fusion protein (a kind gift from Dr. J. Collard) was used as a control. The wt, mutant, and control GST fusion proteins were incubated with ADAM17-Fc overnight at 4°C in binding buffer (50 mM TRIS, 1 mM $CaCl_2$, 1 mM $MgCl_2$, 10% glycerol, 1% Brij-97, pH 7.4) containing protease inhibitors. Protein complexes were pulled down with glutathione-agarose, washed in binding buffer, fractionated in 7.5% SDS-PAGE, transferred to nitrocellulose membranes, and immunoblotted using the commercial H-300 anti-ADAM17 polyclonal antibody. Similarly, levels of pulled-down GST-fusion proteins were assessed by Western blot using commercial anti-GST antibody.

In other experiments, anti-ADAM17 5C2 mAb or anti-human Fc mAb were immobilized in 96-well plates (overnight at 4°C) and ADAM17-Fc or CD69-Fc constructs or whole human IgG3 (at 20 μg/ml) were subsequently captured for 1 h by the respective immobilized antibodies. After washing with 1:10 diluted lysis buffer, cellular lysates (cells were lysed for 30 min at 4°C in HEPES 20 mM-1% Brij-97

containing 1 mM $CaCl_2$, 1 mM $MgCl_2$ and protease inhibitors) of Colo320 and Colo320-CD9 cells were added and protein interactions allowed for 2 h at RT. In reverse studies, plates were first coated with the VJ1/20 anti-CD9 mAb and Colo320 or Colo320-CD9 cellular lysates were subsequently added; excess non-bound material washed and ADAM17-Fc protein was added. After extensive washing, well content was removed with boiling Laemmli buffer and CD9/ADAM17 interactions were detected after resolving in 10% SDS-PAGE under non-reducing conditions and transference to nitrocellulose membranes. For each condition, membranes were incubated using specific anti-ADAM17 (H-300), anti-human Fc, and anti-CD9 (VJ1/20) Abs followed by incubation with secondary HRP-coupled antibodies and ECL detection.

Stimulated release of TNF-α and ICAM-1

Released human TNF-α into the culture medium was determined by ELISA (Immunotools GmbH, Friesoythe, Germany). For phorbol ester-stimulation, 7×10^5 THP-1 cells were seeded in 24-well plates in the presence or absence of 20 ng/ml PMA for 24 h. In some experiments, 20 μg/ml of control (PAINS19, anti-CD59 mAb; PAINS 18, anti-HSPA8; 5A6, anti-CD81; TS82, anti-CD82; Lia 1/1, anti-CD151) or anti-CD9 antibodies (VJ1/20, VJ1/10, or PAINS-13) or ADAM17 inhibitor TAPI-2 (20 or 50 μM) were present during cell treatment with PMA. For HUT78:THP-1 contact stimulation [27], HUT78 cells were stimulated with PHA (1 μg/ml) and PMA (5 ng/ml) for 24 h, fixed in 4% paraformaldehyde and washed extensively with PBS. THP-1 cells were co-cultured with fixed HUT78 cells (at a ratio 1:8) in the presence or absence of anti-CD9 mAbs (VJ1/20, VJ1/10). For THP-1:PBLs contact stimulation [21], PBLs were pre-incubated for 24 h with IL-15 (50 ng/ml) and PBL:THP-1 cells co-cultured at a ratio 10:1 in the presence or absence of specific anti-CD9 mAbs. As a control, PBL:THP-1 cell contact was prevented using 0.4-μm pore-size transwell inserts (Costar).

The amount of ICAM-1 released from THP-1 or Jurkat cells was determined by ELISA with the ICAM Eli-pair kit from Diaclone (Tepnel Life Sciences, France).

Reverse transcription-quantitative polymerase chain reaction for TNF-α

THP-1 (10^6 cells) were seeded in 24-well plates in the absence or presence of PMA (20 ng/ml) or anti-CD9 mAb VJ1/20 (20 μg/ml). After 24 h, cells were washed and lysed, and total RNA was purified using the RNAqueous system (Ambion). Complementary DNA was prepared at a final concentration of 10 ng/μl using the High Capacity Archive kit (Applied Biosystems) and 0.5 ng was amplified in triplicate for TNF-α (and for GAPD expression, used as endogenous reference gene), using specific TaqMan probes (Hs00174128_m1 and Hs99999905_m1 for TNF-α and GAPD, respectively) in a ABI PRISM 7900HT (Applied Biosystems). Data were analyzed with the SDS 2.2.2 software and RQ calculated using deltaCt method.

ICAM-1 shedding measurements from Colo320 cells and Colo320 stable transfectants

Colo320 colon carcinoma cells and the different stable transfectants were transiently transfected with ICAM-1-GFP cDNA in an ElectroSquarePorator ECM 830 as described previously [20, 22]. After 24 h in culture, cells were either treated with PMA (20 ng/ml) for 1 h or left untreated and stained with the anti-ICAM-1 mAb Hu5/3 recognizing an extracellular epitope of ICAM-1, followed by an anti-mouse-APC antibody, to detect intact (uncleaved) transmembrane ICAM-1 expression by flow cytometry. For each Colo320 transfectant, the amount of intact membrane ICAM-1 after PMA treatment was normalized to its level in resting cells to give an indication of ADAM17 activity, and corrected for the changes in the GFP channel, which were in all cases negligible.

Gene knock-down assays

The following shRNAs (OriGene Technologies, Rockville, MD) were stably delivered into THP-1 or Jurkat cells by retroviral infection according to manufacturer's instructions: TR20003 ("TR2") is a control plasmid without shRNA cassette insert; T364190 ("#90") and TI364192 ("#92") are plasmids containing shRNA inserts to knock-down ADAM17; and TI356235 ("#35") is a plasmid with the shRNA insert to silence CD9. Retrovirally transduced cells were selected in puromycin-containing medium and, after 1–2 weeks, reduced expression of ADAM17 or CD9 was assessed by flow cytometry.

To knock-down endothelial CD9, small interference (si)RNA was performed as previously described [20]. HUVECs were stimulated with TNF-α (20 ng/ml) (R&D Systems, Minneapolis, MN) for 20 h before the assays were performed. In some cases, 50 μM TAPI-2 TACE inhibitor was added together with TNF-α.

Results

CD9 and ADAM17 associate on monocytic and endothelial cells

To assess the possible relationship between CD9 and ADAM17 on the endothelial microvasculature cell line

HMEC-1 and PMA-treated THP-1 macrophagic cells, we performed double immunofluorescence staining of these molecules followed by confocal microscopy analysis. Partial co-localization of ADAM17 and CD9 was particularly evident at cell–cell contact areas, but was also found in some apical locations on endothelial cells (Fig. 1a). Since co-localization in optical microscopy was suggestive of an association between these molecules taking place on the cell surface, we employed in situ proximity ligation assays (PLAs) as an alternative approach to further evidence the specific interaction of CD9 with ADAM17. PLA signal is only detected when the secondary probes directed against the two molecules are in a short range distance (around 50 nm) that is consistent with molecular interactions. As shown in Fig. 1b, PLA signal suggestive of the interaction of CD9 with ADAM17 was clearly revealed on the surface of both PMA/THP1 and the endothelium-derived cell clone EA-hy926. In agreement with the co-localization results shown in Fig. 1a, the PLA signal was particularly evident at cell–cell contact regions but was also detected on the apical surface of endothelial cells. The same procedure with a very abundant membrane molecule, such as CD147/EMMPRIN did not provide appreciable PLA signal. As a positive control, we also assayed the interaction of CD9 with CD81, as these two tetraspanins are known to interact forming heterodimers and higher-order oligomers on the cell surface [28, 29].

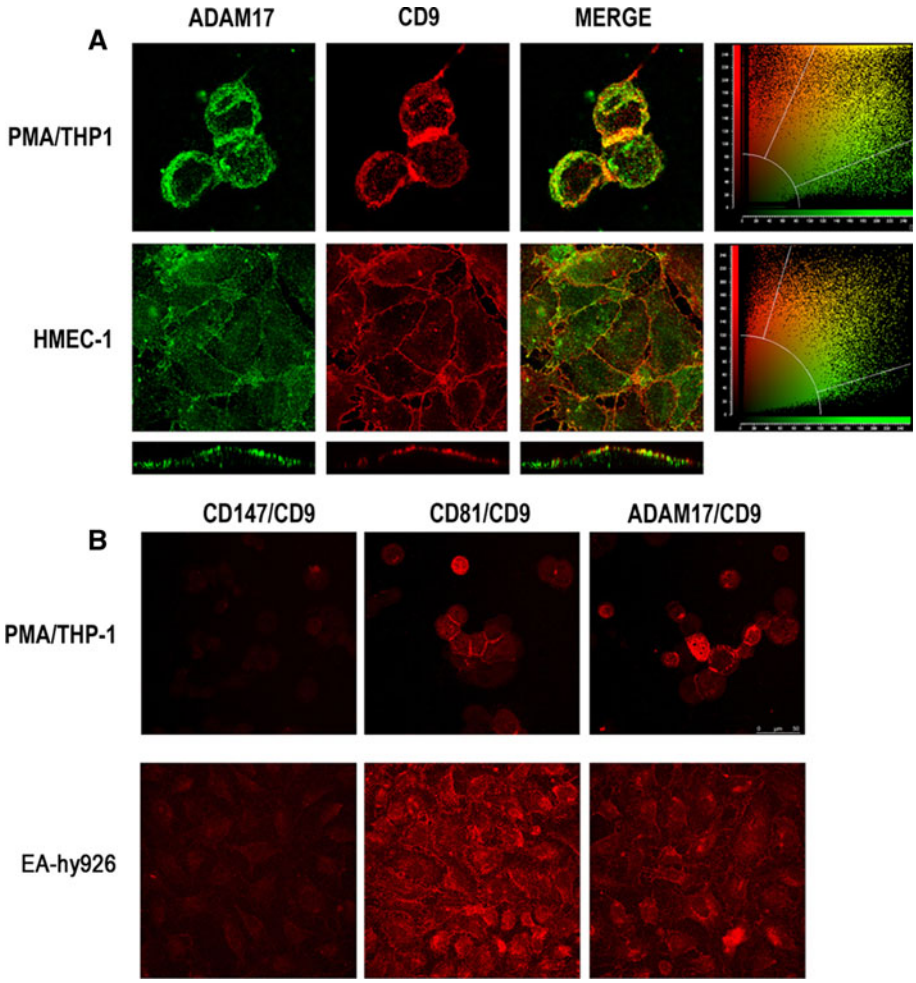

Fig. 1 Confocal microscopy analysis of co-localization and interaction of ADAM17/TACE and CD9 proteins on endothelial and macrophagic cells. **a** Co-localization of ADAM-17 and CD9. PMA-treated THP-1 cells and HMEC-1 cell monolayers were stained with anti-ADAM17 (clone 111633 from R&D Systems) and anti-CD9 (mAb VJ1/20) antibodies. Samples were analyzed by confocal microscopy. Maximal projections of the confocal stack are shown together with merged images and dot-plots of fluorescence depicting intensity quantification in both channels for each pixel of the image (*right panels*). In the case of HMEC-1 cells, vertical sections (z) showing colocalization in the apical cellular surface are shown in the *lower panels*. **b** In situ proximity ligation assays showing molecular interactions between ADAM17 and CD9 on macrophagic PMA-treated THP-1 and endothelial EA-hy926 cells. As a positive control, the interactions between CD81 and CD9 are shown. Negligible interactions between CD147/EMMPRIN and CD9 were detected**.** Maximal projections of the confocal stack are shown

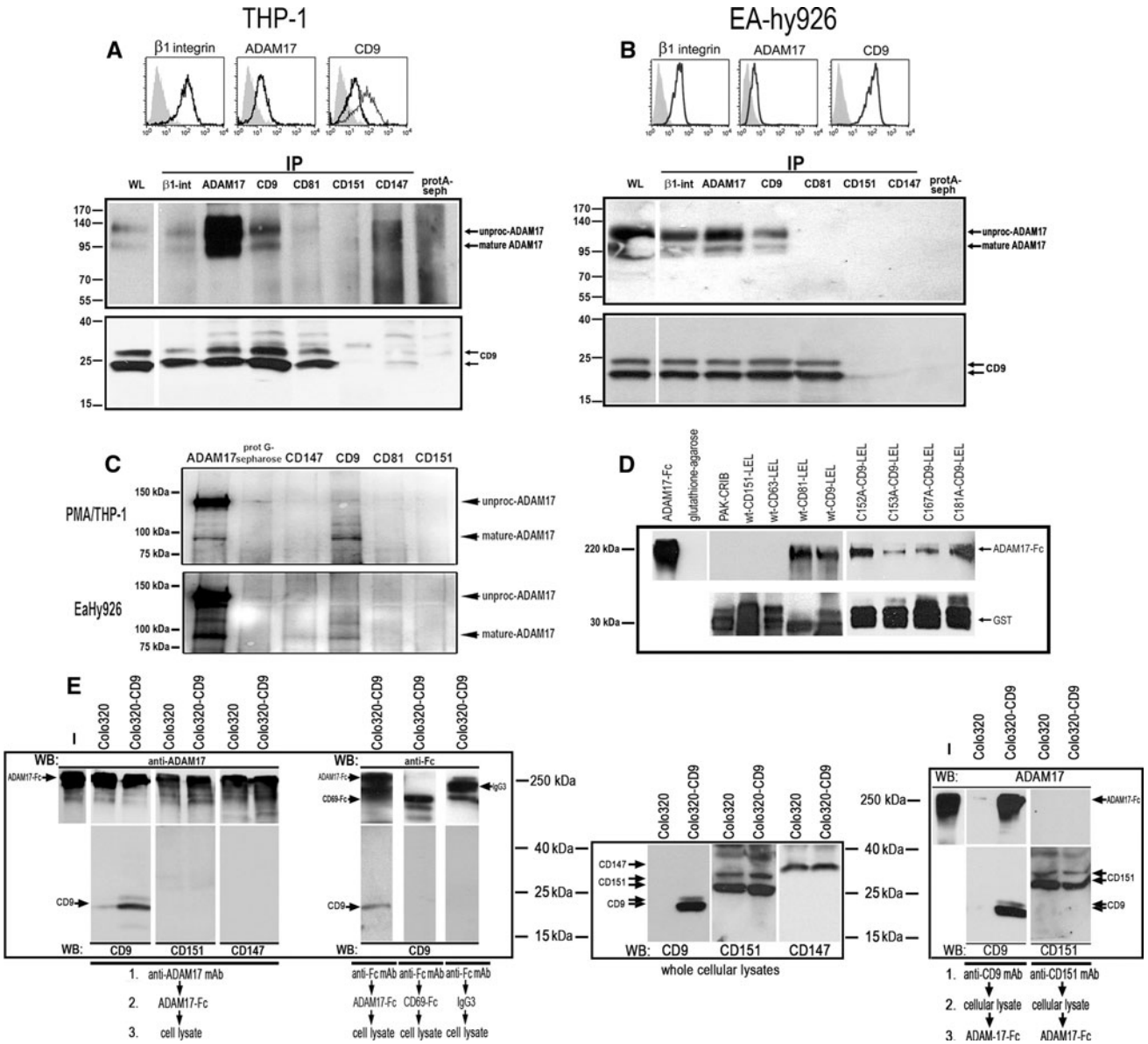

To confirm the possibility that ADAM17 and CD9 could be constituents of the same protein complexes, these molecules were immunoprecipitated from lysates of PMA-treated THP-1 (Fig. 2a) and EA-hy926 (Fig. 2b) cells. CD9 is abundantly expressed on both PMA-differentiated THP-1 macrophage cells and endothelial EA-hy926 cells, whereas the level of ADAM17 surface expression was moderate on both cell lines (Fig. 2a, b, upper panels). As reported [30], we observed an important increase in the surface level of CD9 following treatment of THP-1 cells with PMA (Fig. 2a, upper panel) and thus used these cells for lysis and immunoprecipitation. Cell lysates were prepared under relatively mild solubilization conditions (1% Brij-97) aimed at preserving protein interactions in tetraspanin-enriched microdomains at the plasma membrane. As shown in Fig. 2a and b in the lower panels, two bands of $\approx$130- and $\approx$95-kDa were clearly recognized in whole-cell lysates by the anti-ADAM17 Ab H300. The same two bands were detected when cell lysates were prepared in the presence of the metalloproteinase inhibitors 1, 10-phenanthroline or the hydroxamate TAPI-2, indicating that auto-digestion of the mature form of TACE in these cells is minimal under the lysis conditions employed (data not shown) and that the two detected bands correspond to the unprocessed and mature forms of ADAM17, respectively. Both forms of ADAM17 were specifically co-immunoprecipitated with CD9 and β1 integrin (but not with other tetraspanins such as CD81 or CD151 or with CD147) from PMA-treated THP-1 and EA-hy926 cell lysates. Reciprocally, CD9 was also co-immunoprecipitated with ADAM17 and, as expected, with

◀ **Fig. 2** Biochemical analysis of the association between ADAM17/TACE and the CD9 tetraspanin in monocytic and endothelial cell lines. **a** Surface expression of β1 integrin, TACE/ADAM17, and CD9 molecules in monocytic THP-1 cells was analyzed by flow cytometry *upper panel*. *Grey-filled* histograms correspond to negative control and *thick black line* histograms to the expression of each indicated molecule on untreated cells. For CD9, the level of its expression on PMA-differentiated THP-1 cells is also shown by the *thin-line* histogram. Immunoprecipitation assays from THP-1 cells cultured for 24 h in the presence of 20 ng/ml PMA and lysed using 1% Brij-97 as described in "Materials and methods" *lower panel*. Lysates were immunoprecipitated with anti-β1 integrin (mAb TS2/16), anti-ADAM17 (mAb clone 111633), anti-CD9 (mAb VJ1/20), anti CD81 (mAb 5A6), anti-CD151 (mAb Lia1/1), and anti-CD147 (VJ1/9) antibodies. Immunoprecipitated complexes were resolved in 10% SDS-PAGE under non-reducing conditions. ADAM17 and CD9 were detected by Western blot using H-300 (Santa Cruz Biotechnology) and VJ1/20 antibodies, respectively. Blots are representative of three different experiments. **b** As for THP-1 cells, surface expression of the different molecules was studied in untreated HMEC-1 endothelial cells (*upper panel*). EA-hy926 cells were cultured to confluence and extracted using 1% Brij-97 and immunoprecipitation was carried out as described above. Blots are representative of three different experiments. **c** Surface proteins on PMA-treated THP-1 and EA-hy926 cells were cross-linked with DTSSP prior to lysis in 1% Triton-X100 and cross-linked protein complexes were immunoprecipitated with anti-CD147 (VJ1/9), anti-CD9 (VJ1/20), anti-CD81 (5A6), anti-CD151 (Lia1/1), and anti-ADAM17 (2A10) mAbs. Immunoprecipitated complexes were resolved in 10% SDS-PAGE under reducing conditions to cleave the disulfide bonds of cross-linker. Presence of ADAM17 was identified by immunoblotting with the H-300 pAb (Santa Cruz Biotechnology), which detects both the immature and mature forms of ADAM17 under reducing conditions. **d** Pull-down assays using the wt and C152A, C153A, C167A, or C181A mutant forms of CD9-LEL-GST, wt CD81-LEL-GST, wt CD151-LEL-GST, wtCD63-LEL GST, or the control PAK-CRIB-GST fusion proteins were incubated with ADAM17-Fc as specified under "Materials and methods" (*upper panel*). The *lower panel* shows the immunodetection with an anti-GST antibody of wt and mutant CD9-LEL-GST, wt CD81-LEL-GST, and PAK-CRIB-GST fusion proteins employed. **e** *Left panel*: The 5C2 anti-ADAM17 or anti-human Fc antibodies were first immobilized and ADAM17-Fc, CD69-Fc, or whole human IgG3 then immuno-captured in plastic wells. Lysis buffer (–) or cellular lysates from Colo320 or Colo320-CD9 cells were subsequently added as described in "Materials and methods". The presence/absence of CD9, CD151, and CD147 retained in wells through association with immuno-captured ADAM17-Fc, CD69-Fc, or human IgG3 was probed by immunoblotting with anti-CD9 mAb VJ1/20, anti-CD151 (H-80), or anti-CD147 (VJ1/9) antibodies (*lower blots*). Presence of the immuno-captured ADAM17-Fc or CD69-Fc constructs or whole human IgG3 in the complexes was confirmed by blotting the membranes with the anti-ADAM17 Ab (H-300) and anti-human Fc, respectively, (*upper blots*). *Center panel*: expression of CD9, CD151, and CD147 in whole-cell lysates of Colo320 and Colo320-CD9 cells was confirmed by immunoblotting with respective specific antibodies. *Right panel* Interaction of ADAM17-Fc with cellular CD9 was also confirmed in the reverse experiment in which CD9 or CD151 were first immuno-captured with anti-CD9 (VJ1/20) or anti-CD151 (Lia 1/1) mAbs, respectively, then incubated with lysates of Colo320 or Colo320-CD9 and finally ADAM17-Fc was added to each well. As before, the presence of immuno-captured CD9 or CD151 (*lower blots*) and retained ADAM17-Fc in the protein complexes (*upper blots*) was detected by immunoblotting with specific antibodies

CD81 and β1 integrin. To further confirm that this interaction occurs in the plasma membrane of intact cells, cell surface proteins were cross-linked prior to lysis with the membrane impermeable and thiol-cleavable DTSSP reagent and subsequently immunoprecipitated with anti-ADAM17, antibodies against the tetraspanins CD9, CD81, and CD151 or against another abundant membrane molecules such as CD147 from PMA-treated THP-1 and EA-hy-926 cells. As shown in Fig. 2c, bands corresponding to the mature form of ADAM17 were clearly detected in CD9 immunoprecipitates from both cell types, demonstrating the cross-linking between these two associated proteins on the cell surface. In contrast, negligible cross-linking between ADAM17 and either CD147 or tetraspanins CD81 and CD151 was detected, although these molecules were efficiently immunoprecipitated (Supplemental Fig. 1), indicating the specificity of the CD9/ADAM17 interaction.

Most CD9 lateral interactions with surface proteins involve its large extracellular loop (LEL) [14]. Fusion proteins corresponding to the CD9 LEL domain fused to GST (wt-CD9-LEL) and to the whole extracellular ADAM17 domain fused to the Fc region of human IgG (ADAM17-Fc) were employed to assess direct association of CD9 and ADAM17. ADAM17-Fc was efficiently pulled-down with wt CD9 LEL (Fig. 2d). Interaction of ADAM17-Fc with the wt LEL of CD81—a tetraspanin closely related to CD9—was also clearly detected, but not with the wt LEL of two other tetraspanins, CD151 and CD63, or with the control fusion PAK-CRIB-GST protein. Interestingly, four CD9 LEL-GST constructs in which cysteines C152, C153, C167, or C181 (that are involved in the formation of two intra-LEL domain disulfide bonds) were mutated to alanines retained—although to varying degrees—the ability to pull-down ADAM17-Fc, with C153A and C167A mutants clearly showing markedly reduced interaction.

To confirm association with cellular CD9, ADAM17-Fc was first immuno-captured on plastic wells with an immobilized anti-ADAM17 mAb and then cell lysates of Colo320 (a CD9-negative colon carcinoma cell line) or Colo320-CD9 cells (expressing high amounts of CD9 after stable transfection) were added to wells. After incubation and extensive washing of unbound material and solubilization in Laemmli buffer, CD9 interacting with captured ADAM17-Fc was detected by immunoblotting with mAb VJ1/20. CD9 was clearly detected only when cell lysates of Colo320-CD9 but not of CD9-negative parental Colo320 cells were added into the wells (Fig. 2e, left panel). In contrast, no interaction of immuno-captured ADAM17-Fc with other cellular molecules, such as the tetraspanin CD151 or CD147/EMMPRIN, could be detected although these proteins are highly expressed in both Colo320 and Colo320-CD9 cells as revealed by immunoblotting of

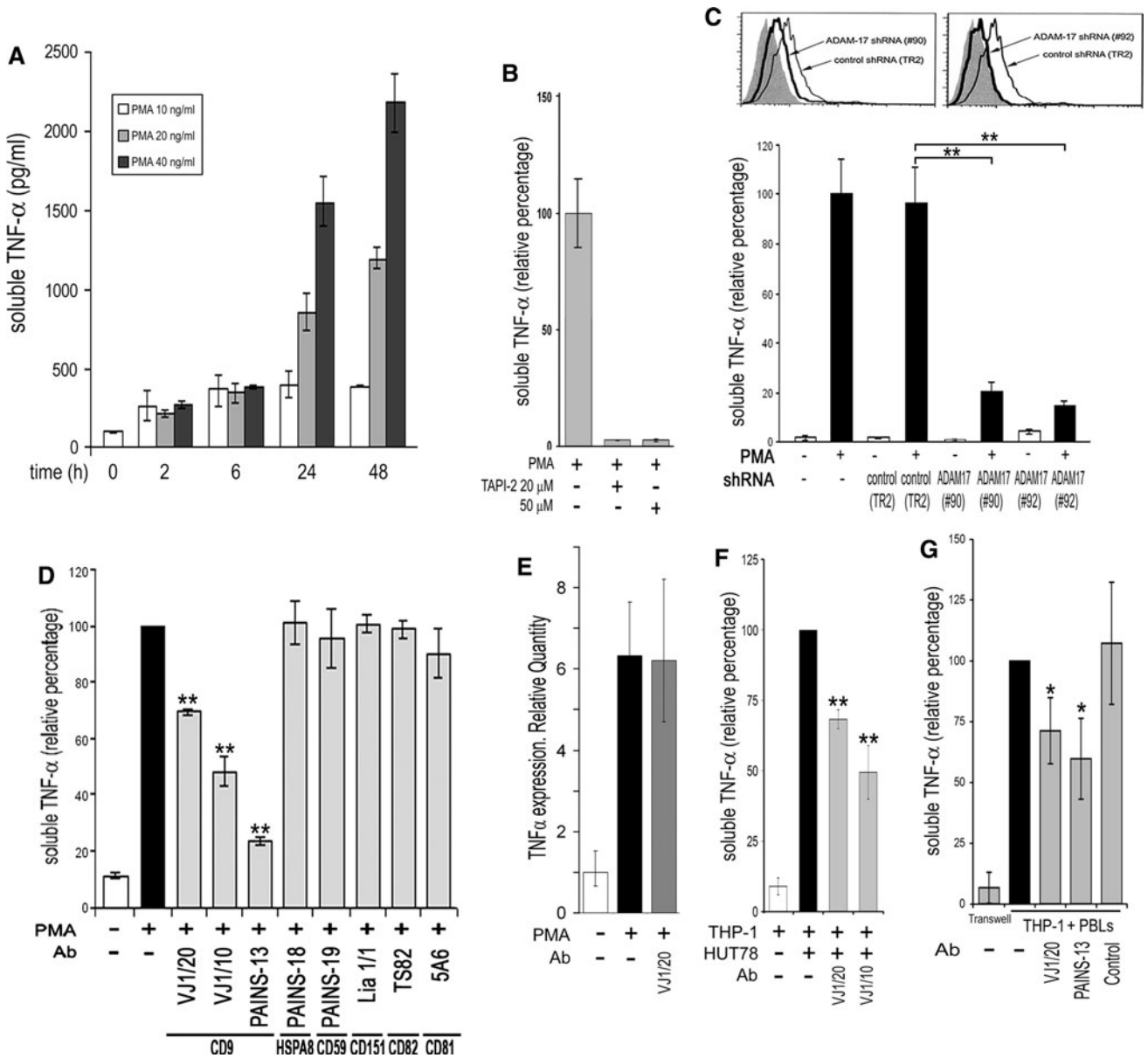

whole-cell lysates (Fig. 2e, center panel) and flow cytometry (not shown). Two additional immuno-captured proteins containing Fc domains, whole human IgG3 and CD69-Fc, did not show interaction with CD9 from Colo320-CD9 lysates, confirming the specificity of the CD9-ADAM17 interaction in these assays and ruling out any non-specific interaction of CD9 with the Fc region (Fig. 2e, left panel).

The interaction of ADAM17-Fc with cellular CD9 was also confirmed in reverse experiments, in which CD9 was first immuno-captured in wells with immobilized mAb VJ1/20 from lysates of Colo320 or Colo320-CD9, excess unbound material washed and finally ADAM17-Fc added. ADAM17-Fc was only retained and immunodetected when CD9 from Colo320-CD9 cells had been previously immuno-captured in the wells (Fig. 2e, right panel). No interaction of ADAM17-Fc with immuno-captured CD151 could be detected in these assays, again indicating the specificity of the ADAM17/CD9 interaction.

Taken together, the co-localization, in situ proximity ligation assays and biochemical results demonstrate the specific and direct interaction on the cell surface of ADAM17 with CD9 through its LEL domain.

Anti-CD9 antibodies inhibit the sheddase activity of ADAM17/TACE

We investigated whether ADAM17 proteolytic activity is regulated through the associated CD9 molecules. THP-1 cells represent a useful system to study regulation of

◀ **Fig. 3** Effects of anti-CD9 mAbs on the ADAM17-mediated shedding of TNF-α from THP-1 cells. **a** ELISA quantification of soluble TNF-α released from THP-1 cells stimulated with different concentrations of PMA for the indicated times. Released TNF-α concentrations were calculated from a standard curve using known amounts of this cytokine. **b** Specific involvement of ADAM17/TACE in the PMA-stimulated (20 ng/ml, 24 h) release of TNF-α from THP-1 cells was assessed using the inhibitor TAPI-2. The amount of soluble TNF-α released from PMA-stimulated cells was considered as 100%. A representative experiment out of five is shown**. c** ADAM17 knock-down abrogates the PMA-stimulated release of TNF-α from THP-1 cells. *Upper panel*: Flow cytometry analysis of ADAM17 expression; *grey-filled* histograms represent unstained control cells, *thin black line* histograms represent THP-1 cells retrovirally transduced with control shRNA plasmid ("TR2") and *thick black line* histograms represent THP-1 cells retrovirally transduced with two different ADAM17-specific shRNA plasmids ("#90" and "#92"). Cells were stained with the anti-ADAM17 Ab H-170. *Lower panel*: TNF-α released by untransduced cells or retrovirally transduced with control shRNA ("TR2") or ADAM17 plasmids ("#90" and "#92"). Cells were treated or not with 20 ng/ml PMA for 24 h and soluble TNF-α was detected by ELISA, as described in "Materials and methods". Soluble TNF-α released from control untransduced cells stimulated with PMA was considered as 100%. Data represent one representative experiment out of five. **d** Soluble TNF-α released from untreated or PMA-stimulated THP-1 cells in the presence of different anti-CD9 or control mAbs. The amount of released TNF-α was expressed as a percentage of the TNF-α released by PMA-stimulated THP-1 cells in the absence of any antibody. Experiments were performed in triplicates and data represent the mean ± SD from five experiments. **e** TNF-α expression was detected by real-time PCR. Data represent relative quantity of TNF-α expression in samples treated for 24 h with PMA alone or PMA plus anti-CD9 mAb VJ1/20 as compared to untreated THP-1 cells. *Error bars* represent the confidence interval of each RQ value with the confidence limit set at 95%. **f** TNF-α released from THP-1 cells activated by contact with HUT78 T cells. THP-1 cells were plated alone or co-cultured with fixed HUT78 T cells for 24 h in the absence or presence of 20 μg/ml of the anti-CD9 mAbs VJ1/20 or VJ1/10. The amount of soluble TNF-α in the culture medium was measured by ELISA and expressed as a percentage of the TNF-α released by the THP-1 cells co-cultured with HUT78 in the absence of antibodies. Data is mean ± SD from one representative experiment out of four. **g** Release of TNF-α from THP-1 cells following stimulation through contact with peripheral blood leukocytes (PBLs). PBLs were incubated with IL-15 (50 ng/ml) for 24 h and then washed and co-cultured together with human THP-1 cells for 24 h in presence of control or anti-CD9. As a negative control, cellular contact between PBLs and THP-1 cells was prevented by separating both cell types using a 0.4-μm pore transwell insert. The amount of TNF-α in the THP-1-PBL condition was considered as the 100% for data calculation. Experiments were performed in triplicates and data is the mean ± SD from four independent experiments. In all cases, **($p < 0.001$) and *($p < 0.01$) denote statistically significant differences in the release of TNF-α, as determined by two-way ANOVA analysis

ADAM17 activity as their treatment with PMA stimulates ADAM17, increasing shedding of the ectodomains of TNF-α and several other ADAM17 substrates [31, 32]. As shown in Fig. 3a, the constitutive release of TNF-α from unstimulated THP-1 cells (time = 0 h) was only minimally above the detection limit of the ELISA employed. An increase in the amount of soluble TNF-α could be detected already after 2 h and 6 h of PMA treatment but was much more evident after 24 h treatment with 20 ng/ml PMA. Higher concentrations and longer PMA exposure further stimulated the shedding of TNF-α but also resulted in increased cell death (not shown). We therefore selected 20 ng/ml PMA for 24 h as the standard conditions to stimulate TNF-α release from THP-1 cells in subsequent experiments, unless otherwise indicated. Under this stimulation protocol, the release of TNF-α was completely abrogated with the drug TAPI-2, a relatively selective inhibitor of ADAM17 [33, 34] (Fig. 3b), indicating that this metalloproteinase is the main sheddase involved. To definitively demonstrate that ADAM17 is responsible for the PMA-stimulated release of TNF-α from THP-1 cells we knocked it down with specific shRNAs. Figure 3c shows that the PMA-stimulated release of TNF-α from THP-1 cells transduced with two different ADAM17-specific shRNAs was almost completely abrogated compared to either PMA-stimulated un-transduced THP-1 cells or transduced with control shRNA.

We next investigated the effects of anti-CD9 mAbs in this cellular system. As shown in Fig. 3d, significant inhibition of TNF-α release from PMA-stimulated THP-1 cells was caused by the presence of three different anti-CD9 antibodies (VJ1/20, VJ1/10, or PAINS-13) but not by mAbs-specific for other tetraspanins—such as CD82 or CD81—or for the control CD59 or HASP8 molecules that are expressed to similar levels to CD9 on the surface of these cells (not shown). An anti-CD151 mAb was also ineffective at inhibiting the PMA-stimulated release of TNF-α, but in this case the level of expression of this tetraspanin on THP-1 cells was much lower than that of CD9. The effects of anti-CD9 mAbs did neither relate to an effect on TNF-α transcription, as confirmed by quantitative real-time PCR (Fig. 3e), nor to an effect on TACE internalization (Supplemental Fig. 2).

More physiological models using T cell contact instead of PMA to stimulate TNF-α release from THP-1 cells have also been described [21, 27]; by employing models with HUT78 T cells (Fig. 3f) or IL-15-treated PBLs (Fig. 3g) as stimuli, we observed similar inhibitory effects of anti-CD9 mAbs on TNF-α release from THP-1 cells.

The observed inhibitory effect of the three anti-CD9 mAbs used in the present study (VJ1/20, VJ1/10, and PAINS13) on the TNF-α release from PMA-stimulated THP-1 cells (Fig. 3d), which is dependent on ADAM17, is in marked contrast to the stimulatory effect exerted by a different set of three anti-CD9 mAbs (SYB-1, ALB-6, and TS9) on the ADAM10-mediated release of TNF-α from unstimulated CD9-transfected Raji cells (Raji/CD9), reported by Arduise et al. [19]. As shown in Fig. 4, our three CD9 mAbs inhibited the release of TNF-α from PMA-stimulated Raji/CD9 cells (which is mediated by ADAM17, as reported by Arduise et al.) but in agreement

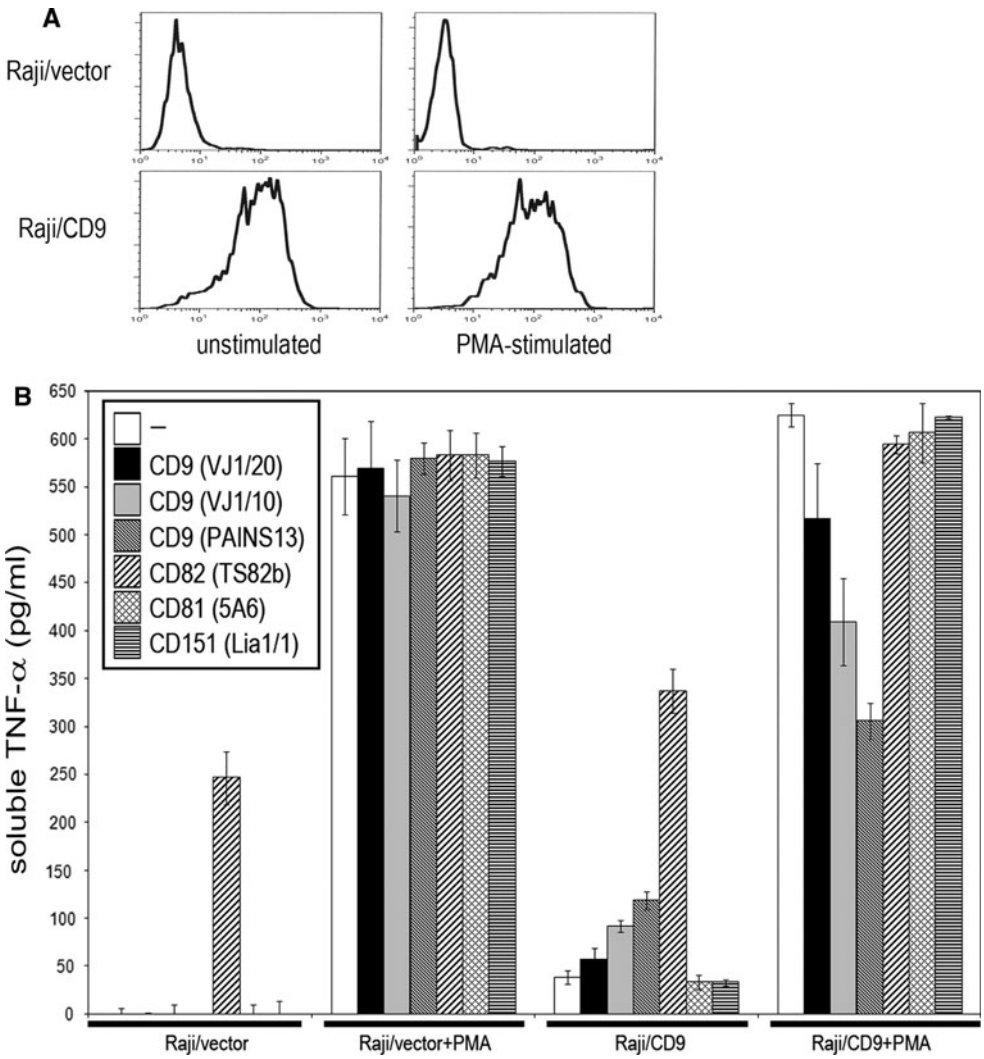

Fig. 4 Effects of anti-tetraspanin mAbs on the ADAM10 and ADAM17-mediated shedding of TNF-α from Raji/CD9 cells. **a** Flow cytometry detection of CD9 expressed on the cell surface of mock-transfected (Raji/vector) and CD9-tranfected Raji (Raji/CD9) cells under unstimulated or PMA-stimulated (40 ng/ml PMA, 24 h) conditions. **b** Quantification of soluble TNF-α released from CD9-negative Raji/vector and CD9-transfected Raji/CD9 cells under resting or PMA-stimulated conditions (40 ng/ml PMA, 24 h) in the absence or presence of the indicated tetraspanin-specific mAbs (20 μg/ml, 24 h). The amount of released TNF-α was measured by ELISA and is expressed in pg/ml. Experiments were performed in triplicates and *bars* represent the mean ± SD. A representative experiment out of three is shown

with the findings already reported [19] with the other anti-CD9 mAbs (SYB-1, ALB-6, and TS9) induced the release of TNF-α from unstimulated Raji/CD9 cells (which, as reported by Arduise et al., is mediated by ADAM10). These data suggest that CD9 mAb inversely regulate ADAM-10 and ADAM-17 activity.

shRNA knocking-down or ectopic neoexpression of CD9 inversely regulate ADAM17 activity in different cell types

Previously, we have described that the anti-CD9 mAbs used in this study act as agonists of CD9 on cell adhesion and proliferation [12]; therefore the inhibition of TNF-α release from PMA-stimulated THP-1 cells caused by these anti-CD9 mAbs points to a negative role of CD9 on ADAM17 activity. To confirm this issue, we assessed the PMA-stimulated shedding of TNF-α after silencing CD9 expression in THP-1 as well as in Jurkat T cells [35, 36]. A significant reduction in membrane expression of CD9 was achieved in both cells (Fig. 5a, b, top panels) after retroviral transduction of specific CD9 shRNA. Interestingly, the PMA-stimulated release of TNF-α was significantly increased in CD9 shRNA interfered cells compared to cells transduced with the control shRNA. This increased PMA-stimulated TNF-α release was not due to enhanced ADAM17 expression as assessed by flow cytometry (data not shown). PMA-induced release of TNF-α in both THP-1 and Jurkat cells was totally dependent on ADAM17 activity as it was almost completely blocked by treatment with the inhibitor TAPI-2 (Fig. 5a, b, middle panels) or TACE silencing (Fig. 5a, b, bottom panels). Noteworthy, the enhanced release of TNF-α from CD9-interfered THP-1 and Jurkat cells correlated with a decrease in transmembrane levels of this cytokine on the same cells (as measured by flow cytometry), which were restored by treatment with TAPI-2, as would be expected from an ADAM-mediated shedding mechanism (Fig. 5 a, b, center panels).

We next investigated if the effect of CD9 silencing on ADAM17-mediated shedding of TNF-α from THP-1 and

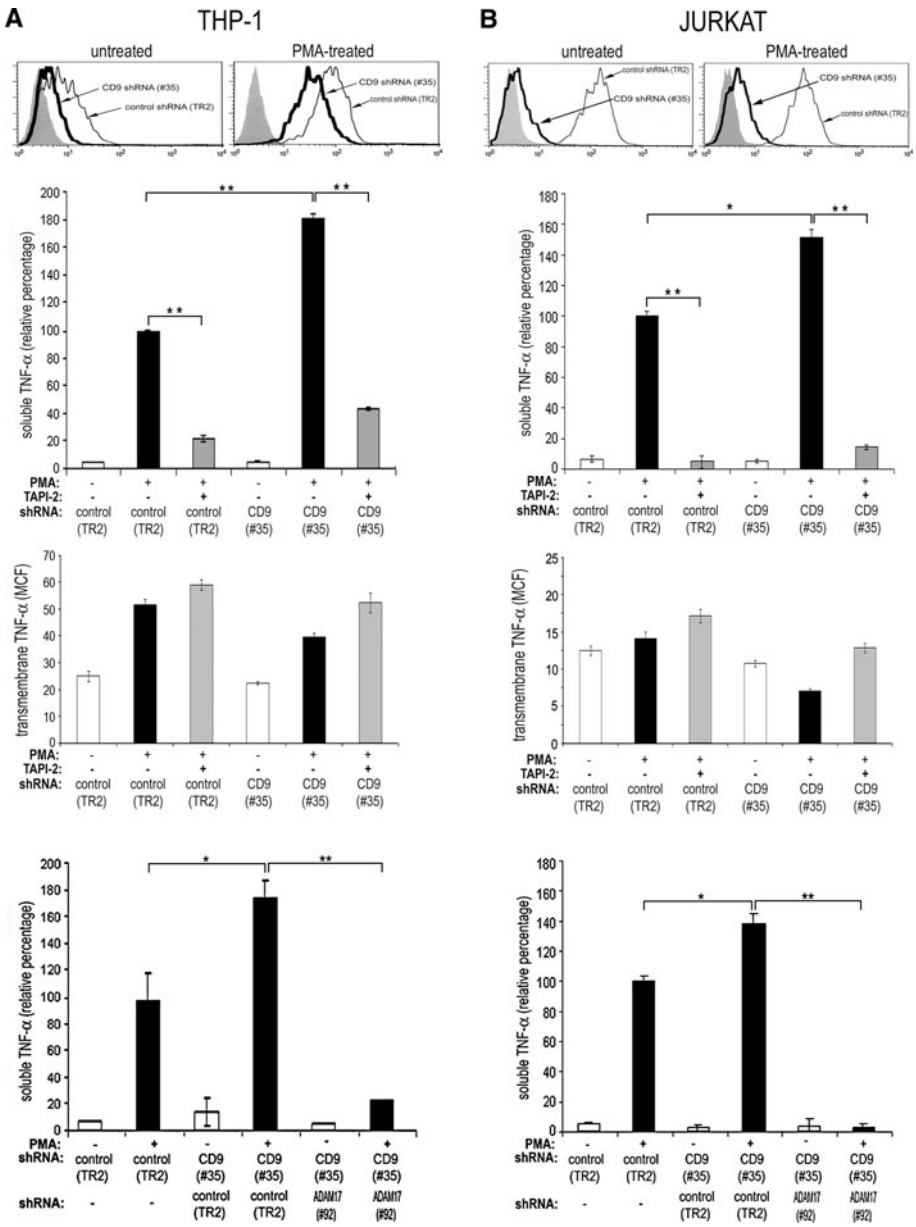

Fig. 5 Effects of shRNA CD9 knock-down on the shedding of TNF-α. Expression of membrane CD9 on THP-1 (**a**, *upper panel*) and Jurkat cells (**b**, *upper panel*) was determined by flow cytometry before and after treatment with 20 ng/ml PMA for 24 h. *Grey-filled* histograms correspond to cells labeled with a negative control antibody, *thin black lines* show the expression of CD9 on cells retrovirally transduced with control shRNA plasmid ("TR2"), and the *thick black lines* show the expression of CD9 on cells stably transduced with shRNA plasmid specific for CD9 ("#35"). *Middle panels*: Amount of released and transmembrane TNF-α from THP-1 (**a**) or Jurkat cells (**b**) retrovirally transduced with a control shRNA plasmid ("TR2") or with a CD9 shRNA plasmid ("#35"). Cells were either untreated or treated for 24 h with 20 ng/ml PMA (THP-1 cells) or 50 ng/ml (Jurkat cells), in the presence or absence of inhibitor TAPI-2 (50 μM). Soluble TNF-α released by control shRNA cells following stimulation with PMA was considered as 100%. Data is mean ± SE from one representative experiment out of eight. Transmembrane levels of TNF-α, expressed as the mean channel fluorescence (MCF), were determined by flow cytometry. Cells retrovirally transduced with control shRNA ("TR2") or CD9-specific shRNA ("#35") were either left untreated or stimulated for 24 h with 20 ng/ml PMA (THP-1 cells) or 50 ng/ml (Jurkat cells) in the presence or absence of the inhibitor TAPI-2 (50 μM). *Lower panels*: Amount of released TNF-α from THP-1 (**a**) or Jurkat (**b**) cells retrovirally transduced with a control shRNA plasmid ("TR2") or with a CD9 shRNA plasmid ("#35"). These stably CD9-silenced cells ("#35") were additionally transiently transfected either with control shRNA ("TR2") or with ADAM17 shRNA plasmid ("92"). Cells were either left untreated or treated for 24 h with 20 ng/ml PMA (THP-1 cells) or 50 ng/ml (Jurkat cells). Data correspond to one representative experiment out of three. In all cases, **($p < 0.001$) and *($p < 0.01$) denote statistically significant differences, as determined by two-way ANOVA analysis

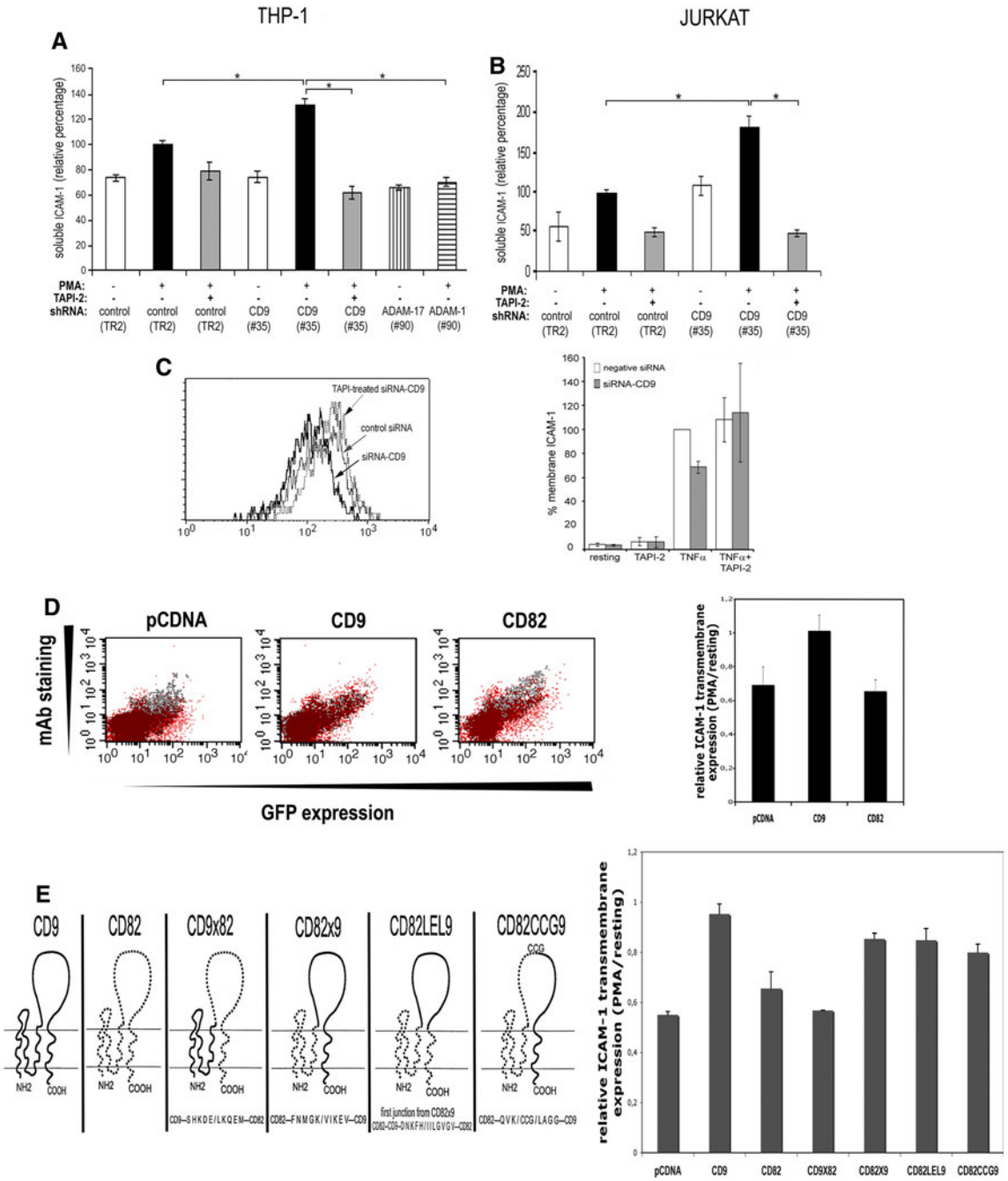

Jurkat cells also applied to ICAM-1, another relevant substrate of this metalloproteinase [4]. As shown in Fig. 6a and b, the PMA-stimulated release of ICAM-1 from CD9-silenced THP-1 cells or Jurkat T was significantly increased compared to that from control-interfered cells. ICAM-1 release was abrogated by TAPI-2, indicating its dependence on ADAM17 activity, which was further demonstrated by the blockade of ICAM-1 shedding observed in ADAM17-silenced cells.

We have reported that diminished transmembrane ICAM-1 expression on TNF-α-stimulated HUVECs occurs after CD9 silencing, with functional consequences in leukocyte adherence and extravasation [20]. Therefore, we investigated whether the observed reduction in ICAM-1 surface expression on CD9-interfered endothelial cells could be mediated by ADAM17. Figure 6c shows that the reduction in the expression of surface ICAM-1 observed on TNF-α-stimulated HUVECs after siRNA-CD9 was reverted by treatment of cells with TAPI-2, whereas the levels of ADAM17 detected by flow cytometry were not altered by siRNA-CD9 or TAPI-2 treatment (data not shown).

Considering the effect of CD9 on ADAM17 activity observed in different cell systems, we reasoned that inhibitory effects should also occur following ectopic

◀ **Fig. 6** Effects of knocking down and ectopic neoexpression of CD9 on the ADAM17-mediated shedding of ICAM-1. The amount of soluble ICAM-1 released from THP-1 cells stimulated for 24 h with 20 ng/ml PMA (**a**) and from Jurkat cells stimulated for 24 h with 50 ng/ml PMA (**b**) was determined by ELISA. Cells were retrovirally transduced with a control shRNA plasmid ("TR2") or with a CD9-specific shRNA plasmid ("#35"). The dependence of ICAM-1 release upon ADAM17 metalloproteinase activity was assessed by treating cells with the inhibitor TAPI-2 (50 μM) and by knocking-down ADAM17 expression with a specific shRNA plasmid ("#90"). The amount of soluble ICAM-1 released from cells retrovirally transduced with control plasmid ("TR2") upon stimulation with PMA was considered as 100%. Data represent the means ± SD from one representative experiment out of five. **c** siRNA knocking-down of CD9 in HUVECs results in diminished levels of membrane ICAM-1. Selective knock-down expression of endothelial tetraspanin CD9 by siRNA assay was performed as described in "Materials and methods". Cells were cultured onto fibronectin to confluence in the absence (resting) or in the presence of TNF-α for 20 h. Dependence of ICAM-1 shedding on ADAM17 activity was assayed by addition of the inhibitor TAPI-2 (50 μM) for 20 h. *Left panel*: Surface expression of ICAM-1 was analyzed by flow cytometry using the Hu5/3 mAb as primary antibody in TNF-α–treated control siRNA interfered-HUVECs (*thin line*), CD9 siRNA interfered HUVECs (*thick line*) and CD9 siRNA interfered in the presence of TAPI-2 (*dotted line*). *Right panel*: Relative amounts of membrane ICAM-1 were calculated from the mean fluorescence intensity, considering the value obtained for TNF-α-treated control siRNA-interfered HUVEC cells as 100%. Data represent the mean ± SD of two independent experiments. **d** Ectopic neo-expression of CD9 (but not of CD82) in colon carcinoma cell line Colo320 inhibits PMA-induced ICAM-1 shedding. *Left panels*: cDNA for ICAM-1-GFP was transiently transfected in Colo320 cells stably transfected with either empty vector (pCDNA3) or with vector containing the cDNA coding for CD9 or for CD82. Cells were stained with the anti-ICAM-1 mAb Hu5/3 followed by an anti-mouse-APC antibody to detect intact transmembrane ICAM-1 expression by flow cytometry. Dot-plots show the cell distribution in terms of fluorescence corresponding to the GFP expression (*x*-axis) and to intact transmembrane ICAM-1 expression (*y*-axis) prior (*grey dots*) or after (*red dots*) their treatment for 1 h with PMA (20 ng/ml). ICAM-1 shedding is reflected by the displacement of dots from a diagonal distribution towards high GFP fluorescence/low intact ICAM-1 expression in pCDNA3 and CD82-transfected cells. The PMA-induced displacement is not observed in CD9-expressing cells reflecting the inhibition of ICAM-1 shedding. *Right panel*: Bars represent the ratios of expression of intact transmembrane ICAM-1 (mean fluorescence intensity of Hu5/3 mAb staining) after/before PMA treatment, as an indication of TACE/ADAM17-mediated shedding. Data represent the mean ± SD of triplicate samples. **e** Colo320 cells were stably transfected with either empty vector (pCDNA3) or with vector containing the cDNA coding for CD9, for CD82 or for each of the CD9/CD82 chimeric tetraspanin molecules (CD82 × 9, CD9 × 82, CD82LEL9, and CD82CCG9) represented on the left. These stable transfectants were transiently transfected with ICAM-1-GFP. Each cell transfectant was either treated with PMA (20 ng/ml) for 1 h to activate ADAM17 or left untreated and then stained with the anti-ICAM-1 mAb Hu5/3 as in **d**. Data represent the mean ± SD of four independent experiments. *($p < 0.01$) denotes statistically significant differences, as determined by two-way ANOVA analysis

neoexpression of CD9 in cells lacking this tetraspanin. To assess this hypothesis, we selected the human colon carcinoma Colo320 cells (because they lack endogenous expression of tetraspanins CD9 and CD82) and transfectant cell lines derived from them (Colo320-CD9 and Colo320-CD82) [12, 22] (Fig. 6d, left panels). We assessed by immunoblotting and flow cytometry that the levels of ADAM17 were not altered following stable CD9 or CD82 transfection (not shown). Colo320-pCDNA3 (stably transfected with empty vector), Colo320-CD9 and Colo320-CD82 cells were additionally transfected with a cytoplasmic-GFP-tagged ICAM-1 cDNA. ADAM-17-mediated shedding was stimulated by short treatment (1 h) of cells with PMA (20 ng/ml). As shown in Fig. 6d, in the case of Colo320-pCDNA3 and Colo320-CD82, PMA induced a clear shift towards lower expression of intact ICAM-1 (detected with mAb Hu5/3 which is specific for the extracellular region of ICAM-1, red dots [37]), reflecting the shedding of this molecule, compared to the same cells without PMA treatment (gray dots). This shift in the expression of intact transmembrane ICAM-1 did not take place in the case of Colo320-CD9 cells, indicating an inhibition of ADAM17 sheddase activity against ICAM-1 after neoexpression of CD9.

To perform a structure–function analysis with the aim to establish which regions of CD9 are responsible for the observed inhibition of ADAM17 activity, we have made use of a set of Colo320 cell transfectants stably expressing significant amounts of different CD9/CD82 chimeric tetraspanin molecules (CD9x82, CD82x9, CD82LEL9, and CD82CCG9) (Supplemental Fig. 3) [22]. As shown in Fig. 6e, only the tetraspanin molecules containing the CD9 LEL (wtCD9 and chimeras CD82x9, CD82LEL9) displayed clear inhibitory effects on the short-term PMA-stimulated shedding of ICAM-1. In contrast, expression of wtCD82 or the chimeric molecule containing the CD82 LEL (CD9x82) did not show any inhibitory effect. These results establish that the LEL domain of CD9 is responsible for the interaction and functional effects exerted by this tetraspanin on ADAM17 activity and concur with the in vitro pull-down data shown in Fig. 2d. We further narrowed down the region of the CD9 LEL involved in these effects through the use of the CD82CCG9 chimera, whose first part of its LEL corresponds to CD82 (up to the CCG motif) and only the second part of its LEL corresponds to CD9. This chimeric tetraspanin displayed a significant inhibitory effect on ICAM-1 shedding, indicating that the second hypervariable half of CD9 LEL is crucial at mediating the functional effects exerted by this tetraspanin on ADAM17.

Dynamic regulation of the CD9-TACE association by phorbol ester stimulation

The results presented so far clearly show that the tetraspanin CD9 associates with ADAM-17/TACE on the cell surface and through this interaction exerts a negative

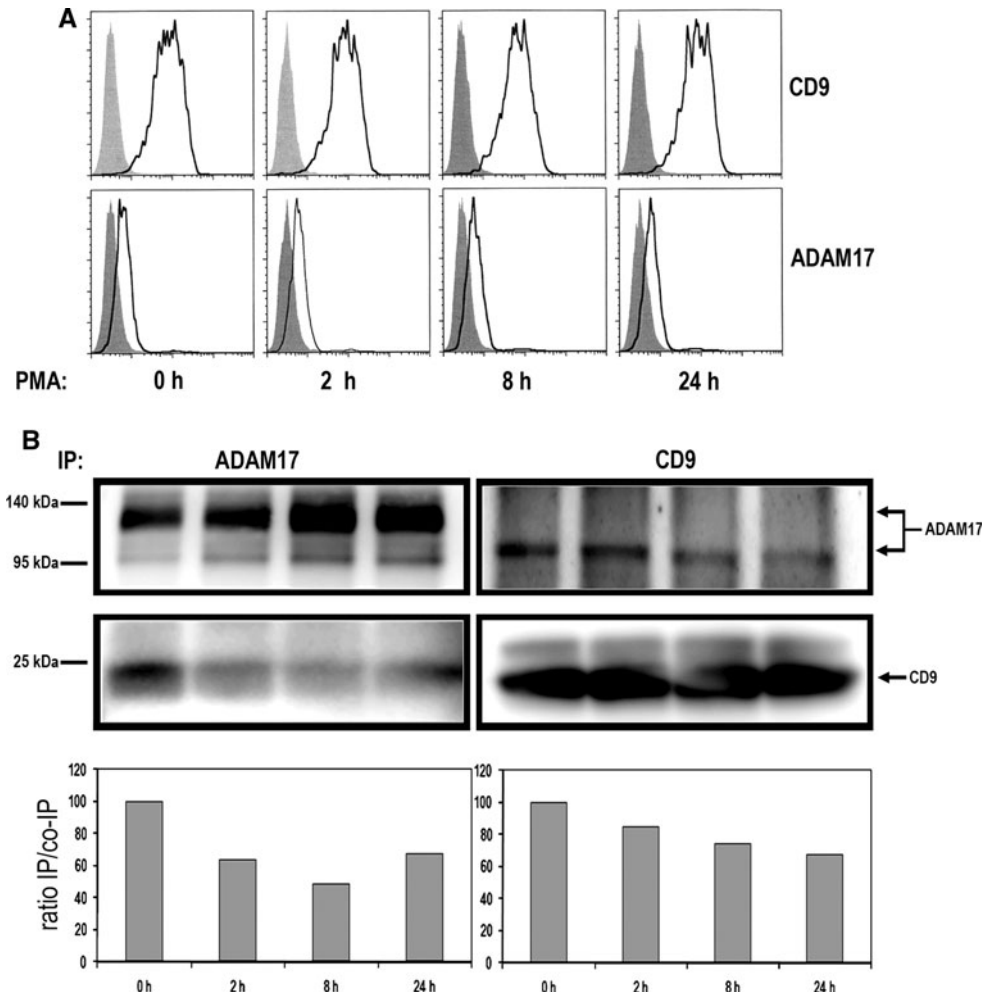

Fig. 7 Association of CD9 with ADAM-17 is dynamically regulated by phorbol ester PMA. **a** Expression of surface CD9 and ADAM17 on endothelial EA-hy926 cells remains stable and is not affected by treatment with 50 ng/ml PMA for the indicated times. **b** *Upper panels*: EA-hy926 cells were treated with PMA (50 ng/ml) for the indicated times, then lysed in 1% Brij-97 and ADAM17 or CD9 immunoprecipitated with 2A10 and VJ1/20 mAbs, respectively, as described in "Materials and methods". The presence of CD9 co-immunoprecipitated with ADAM17 and of ADAM17 co-immunoprecipitated with CD9 were detected by Western blot using VJ1/20 (CD9) and H-300 (ADAM17) antibodies, respectively. *Lower panels*: The ratios between the amount of immunoprecipitated and co-immunoprecipitated proteins were calculated from densitometric analysis of bands as described in "Materials and methods" and represented relative to the ratio from untreated cells (PMA = 0 h), which was considered as 100%. A representative experiment out of two is shown

regulatory role on the sheddase activity of this metalloproteinase. In order to play a functionally relevant role in cellular physiology, this association of CD9 with TACE is expected to be dynamically regulated by intracellular signaling. To evaluate this possibility, we assessed changes in the amount of ADAM-17/TACE and CD9 that co-immunoprecipitated along with immunoprecipitated CD9 and ADAM17, respectively, from EA-hy926 cell lysates following stimulation with phorbol ester PMA (50 ng/ml) for different periods of time (0, 2, 8, and 24 h). The results of these experiments clearly show that the interaction between CD9 and ADAM17 is reduced by PMA stimulation as evidenced by the decreased ratios between immunoprecipitated and co-immunoprecipitated proteins (Fig. 7b). We also checked that these changes in CD9/ADAM17 association were not due to alterations in the level of expression of these proteins (Fig. 7a).

Discussion

ADAM17/TACE is responsible for the shedding of a large variety of transmembrane cell surface proteins, including the cytokine TNF-α and the adhesion molecule ICAM-1, which are critically involved in inflammation and immune responses [2–4]. The process of ADAM17 activation remains largely unknown. Phorbol esters like PMA stimulate ADAM17 activity and concomitant PKC-mediated

phosphorylation of its cytoplasmic tail [2, 38]. However, the activity of a truncated ADAM17 form lacking the cytoplasmic tail is still stimulated by PMA, implying that additional regulatory mechanisms are involved [39]. PMA might alter ADAM17 interaction with other proteins, affecting its sheddase activity. In this regard, PMA modulates the functional interaction of ADAM17 with FHL2, an intracellular protein involved in protein–protein interactions and in their association with actin cytoskeleton [40]. Similarly, the PMA-promoted interaction of ADAM17 with the metalloendopeptidase nardilysin enhanced ADAM17-dependent ectodomain shedding of its substrate HB-EGF [41]. In contrast, other intracellular proteins have been shown to negatively regulate ADAM17 activity through association to its cytoplasmic tail, including SAP97 and PTPH1 [42, 43].

We report here that ADAM17 is a component of surface multiprotein complexes that also comprise CD9 and integrin $\beta 1$ on endothelial and leukocytic cells. This is in agreement with the reported interaction between ADAM17 and integrin $\alpha 5\beta 1$ [26]. The occurrence of these complexes has been demonstrated here by different complementary approaches: co-localization, in situ proximity ligation assays, chemical cross-linking, co-immunoprecipitation, and pull-down experiments employing recombinant proteins.

Interestingly, while both unprocessed and the mature forms of ADAM17 were co-immunoprecipitated with CD9 from monocytic and endothelial cells, almost all ADAM17 found associated to CD9 after chemical cross-linking belonged to the mature form. The fact that the chemical cross-linker employed (DTSSP) is membrane-impermeable indicates that in the plasma membrane CD9 directly interacts mostly with the mature (catalytically active) form of ADAM17. On the other hand, the fact that both forms of ADAM17 are co-immunoprecipitated with CD9 after cell lysis in milder (1% Brij-97) conditions may reflect that ADAM17/CD9 associations take place during maturation of ADAM17 and transit to the plasma membrane.

The specific interaction of the recombinant extracellular domain of ADAM17 with cellular CD9 (but not with other abundantly expressed cell surface proteins) was also detected in lysates of Colo320-CD9 transfected cells, but not of CD9-negative parental Colo320 colon carcinoma cells. It is well established that most tetraspanin interactions with other membrane proteins are mediated by the variable region within their LEL domain, whose conformation is maintained by distinct disulfide bonds [14]. Our protein–protein interaction assays indicate that CD9 directly associates with ADAM17 through its LEL domain. Interestingly, partial loss of the LEL conformation in mutants C153A and C167A, which form one disulfide bridge that extends from the beginning (N-end) to the central region of the variable region of the LEL, dramatically reduced the interaction with ADAM17, whereas mutants in cysteines C152A and C181A, that form a second disulfide bond between the N- and C-ends of the variable region, had only a minor impact on the interaction with ADAM17. In this regard, C152/153 mutations had only a small effect on other CD9-mediated events like HIV uptake [44] and a much larger but still incomplete inhibitory effect on sperm/egg fusion [25]. Similarly, fusion of monocytes to become giant cells was also inhibited by CD9 LEL Cys153 but to only 50% of the maximal inhibition induced by wild-type CD9 LEL. These data suggest that different regions of CD9 LEL mediate distinct functions and only some are sensitive to disruption of disulfide linkages. Further support for the importance of the LEL domain at mediating CD9-mediated functional effects has been obtained through expression of a set of different tetraspanin chimeras, encompassing different regions of CD9 and CD82, in colorectal carcinoma Colo320 cells showing that the inhibitory effects of CD9 on the PMA-stimulated shedding of ICAM-1 requires the CD9 LEL domain. We found that CD81 LEL also interacts with ADAM17 in vitro; this tetraspanin is highly homologous to CD9 and has been recently reported to interact with ADAM10, which is the member of the ADAM family most closely related to ADAM17/TACE [19, 45]. However, in situ crosslinking experiments did not reveal a direct association between CD81 and ADAM17. This apparent paradox might be due to steric constrictions in the plasma membrane, limiting the intermolecular access and direct molecular associations. Moreover, CD9 and CD81 are usually forming heterodimers, so indirect association is feasible. However, mAbs anti-CD81 did not inhibit ADAM17 activity, further suggesting that among these molecules CD9 is the main in vivo modulator of ADAM17-dependent shedding. In contrast, the LELs of two additional tetraspanins, CD151 and CD63, did not show any association with recombinant ADAM17, indicating the specificity of the observed interactions.

We show here that treatment with agonist CD9-specific mAbs or CD9 neoexpression inhibit ADAM17 sheddase activity against its substrates TNF-α and ICAM-1, while CD9 silencing had the opposite effect in leukocytes and endothelial cells. These results would explain the reported increase in membrane TNF-α on different human colon carcinoma cells after neoexpression of CD9 or treatment with anti-CD9 mAbs [12].

We have previously reported that the adhesive function of ICAM-1 and VCAM-1 during leukocyte transendothelial migration is crucially regulated by endothelial tetraspanins [20]. Here we show that CD9 silencing on stimulated HUVEC results in a clear decrease in the membrane level of ICAM-1, likely reflecting the release from the inhibitory effect exerted by CD9 on TACE

activity. The inhibitor TAPI-2 restored the surface levels of ICAM-1 in CD9-interfered HUVEC, suggesting the implication of ADAM17. These results help to explain the mechanism by which CD9 regulates the levels of ICAM-1 on endothelial cells and the subsequent consequences in terms of leukocyte adhesion and transmigration [15, 20].

Compartmentalization within tetraspanin-enriched microdomains (TEMs) is emerging as an important regulatory mechanism of the function of adhesion and signaling receptors and different transmembrane metalloproteinases (reviewed in [13, 46]). The modulation of ADAM17 sheddase activity through association with CD9 described here represents another relevant example of such regulatory mechanisms. Several non-mutually exclusive possibilities could explain the observed negative influence of CD9 on ADAM17 activity. One such possibility is that upon direct interaction with CD9-LEL, conformational changes are imposed to the extracellular region of ADAM17 leading to inhibition of its proteolytic activity. In this regard, conformational changes have been reported to be transmitted to integrin $\alpha 3\beta 1$ upon association with the tetraspanin CD151, resulting in this case in integrin activation and enhanced ligand-binding [47]. Our results also show that intracellular signals can dynamically regulate the extent of association between CD9 and ADAM-17 within TEMs on the cell surface. The observed dissociation between CD9 and ADAM17 that is induced by PMA treatment could partially explain the stimulatory effect of PMA on ADAM17 activity through a mechanism involving its release from the inhibitory effect conferred through CD9 interaction.

Another possibility is that CD9-mediated compartmentalization of either ADAM17 itself or some of its substrates would result in their reduced lateral mobility within the plane of plasma membrane, effectively limiting substrate accessibility to ADAM17 cleavage.

Over-expressed CD9 has been shown to interact with pro-HB-EGF, pro-TGF-α, pro-epiregulin, and pro-amphiregulin, markedly enhancing the juxtacrine signaling mediated by these four transmembrane ligands of EGFR which, in addition, are well-established substrates of ADAM17 (reviewed in [8, 14]). In fact, CD9 has been reported to strongly decrease the PMA-induced proteolytic conversion of transmembrane to soluble TGF-α [48]. The inhibitory effect of CD9 on ADAM17 activity described here would explain the important role of this tetraspanin as an enhancer of EGFR juxtacrine signaling by increasing the surface levels of these transmembrane ligands. CD9 could also potentially inhibit the reported crosstalk between GPCRs and EGFR signaling, which requires release of EGFR ligands by different ADAMs, including ADAM17, and has been shown to contribute to tumorigenesis, migration, and invasion in different tumor cell lines (reviewed in [1, 49]). In this regard, our data would be consistent with the well-established tumor and metastasis-suppressor role of CD9 in a variety of carcinoma types [9, 10, 12, 46].

Arduise et al. [19] elegantly showed that within the context of TEMs, different tetraspanins associate with ADAM10/Kuzbanian, which is the member most closely related to ADAM17 within the ADAM family [1]. Interestingly, they showed that antibody-engagement of specific tetraspanins, including CD9, CD81, and CD82, stimulates EGF and TNF-α release through ADAM10, illustrating another example of functional regulation of ADAM-mediated shedding by associated tetraspanins. The current view on the shedding process maintains that while the constitutive release is mainly mediated by ADAM10, the inducible one is mostly dependent on ADAM17 [50]. In the present study, we have addressed the effects of CD9 expression and anti-CD9 mAbs on PMA-stimulated shedding of TNF-α and ICAM-1 and through silencing of ADAM17 have demonstrated that this stimulated shedding is mediated by this metalloproteinase. Moreover, neoexpression of CD9 and chimeras containing CD9 LEL inhibited PMA-induced ICAM-1 shedding. This shedding was measured at 1 h of PMA treatment, which is a hallmark for ADAM17 function. However, the work of Arduise et al. [19] addressed mostly the effects of anti-tetraspanin antibodies on the constitutive shedding of TNF-α and EGF, which is mainly mediated by ADAM10. This stimulation of ADAM10-mediated shedding of TNF-α caused by anti-tetraspanin antibodies is the opposite to the inhibitory effect of anti-CD9 mAbs on ADAM17 activity that we report here. Our data clearly show that the three anti-CD9 mAbs employed in our study also inhibited the ADAM17-mediated release of TNF-α from PMA-stimulated Raji/CD9 cells (similarly to their effect on PMA-stimulated THP-1 cells) but, in contrast, induced the ADAM10-dependent TNF-α release from resting Raji/CD9 cells, clearly revealing the they exert opposite regulatory effects, stimulatory versus inhibitory, on ADAM10 and ADAM17 activities, respectively. Moreover, the regulatory effects exerted by CD9 on ADAM17 seem to be quite general and do not appear to be restricted to a particular cellular system (we have observed these effects with PMA-THP-1, PMA-Jurkat, and PMA-Raji/CD9 cells) or to a specific ADAM17 substrate (we have observed the effects on the processing of TNF-α and ICAM-1). Although both ADAM10 and ADAM17 share many of their substrates (including EGF and TNF-α, IL6-receptor, and chemokines CXCL1 and CXCL16) the mechanisms controlling their accessibility to, and shedding by, each specific ADAM might however be completely different.

Another interesting example of ADAM regulation by a tetraspanin is the interaction of TSPAN12 with ADAM10 [45]. In this case, ADAM10-dependent shedding of amyloid

precursor protein (APP) is enhanced by TSPAN12 overexpression, while siRNA ablation of TSPAN12 diminished APP proteolysis in different tumor cells; this novel mode of regulating APP cleavage is of obvious relevance to Alzheimer's disease therapy. Finally, functional regulation of the matrix metalloproteinase MT1-MMP through interaction with tetraspanin CD151 on human endothelial cells [51] or through interactions with tetraspanins CD9, CD81, and TSPAN12 on cancer cells [52] has also been described. Therefore, the role of tetraspanins as key regulators of the catalytic activity of different transmembrane metalloproteinases is emerging as a theme of the utmost physiological and pathological relevance, considering the variety and importance of the substrates that are processed by these enzymes.

Acknowledgments We are very grateful to Dr. M. Humphries for providing ADAM17-Fc cDNA; to Mariano Vitón and Sandra Moreno for their technical assistance, and to Dr. Ricardo Ramos-Ruiz for his assistance with the real-time PCR assays. This work was supported by grants BFU2007-66443/BMC and BFU2010-19144/BMC from Ministerio de Ciencia e Innovación, a grant from Fundación de Investigación Médica Mutua Madrileña and by RETICS Program RD08/0075-RIER (*Red de Inflamación y Enfermedades Reumáticas*) from Instituto de Salud Carlos III (to C.C.), a grant from Fundación de Investigación Médica Mutua Madrileña (to M.D.G.L.), and grants PI080794 from Instituto de Salud Carlos III (to M.Y-M) and SAF2007-60578 from Ministerio de Ciencia e Innovación (to E.M.L.). M.D.G.L. was supported by a contract associated to grant SAF2004-01715 from Ministerio de Ciencia e Innovación. S.O. was supported by an I3P predoctoral Fellowship from Consejo Superior de Investigaciones Científicas (CSIC) and by a contract associated to grant BFU2007-66443/BMC from Ministerio de Ciencia e Innovación. A.G. has been supported by a predoctoral Fellowship from Instituto de Salud Carlos III and by grant BFU2007-66443/BMC from Ministerio de Ciencia e Innovación.

References

1. Edwards DR, Handsley MM, Pennington CJ (2008) The ADAM metalloproteinases. Mol Aspects Med 29(5):258–289
2. Mezyk R, Bzowska M, Bereta J (2003) Structure and functions of tumor necrosis factor-alpha converting enzyme. Acta Biochim Pol 50(3):625–645
3. Black RA (2002) Tumor necrosis factor-alpha converting enzyme. Int J Biochem Cell Biol 34(1):1–5
4. Tsakadze NL, Sithu SD, Sen U, English WR, Murphy G, D'Souza SE (2006) Tumor necrosis factor-alpha-converting enzyme (TACE/ADAM-17) mediates the ectodomain cleavage of intercellular adhesion molecule-1 (ICAM-1). J Biol Chem 281(6):3157–3164
5. Garton KJ, Gough PJ, Raines EW (2006) Emerging roles for ectodomain shedding in the regulation of inflammatory responses. J Leukoc Biol 79(6):1105–1116
6. Gearing AJ, Newman W (1993) Circulating adhesion molecules in disease. Immunol Today 14(10):506–512
7. Jackson LF, Qiu TH, Sunnarborg SW, Chang A, Zhang C, Patterson C, Lee DC (2003) Defective valvulogenesis in HB-EGF and TACE-null mice is associated with aberrant BMP signaling. EMBO J 22(11):2704–2716
8. Murphy G (2009) Regulation of the proteolytic disintegrin metalloproteinases, the 'Sheddases'. Semin Cell Dev Biol 20(2):138–145
9. Miyake M, Inufusa H, Adachi M, Ishida H, Hashida H, Tokuhara T, Kakehi Y (2000) Suppression of pulmonary metastasis using adenovirally motility related protein-1 (MRP-1/CD9) gene delivery. Oncogene 19(46):5221–5226
10. Miyake M, Nakano K, Itoi SI, Koh T, Taki T (1996) Motility-related protein-1 (MRP-1/CD9) reduction as a factor of poor prognosis in breast cancer. Cancer Res 56(6):1244–1249
11. Chen MS, Tung KS, Coonrod SA, Takahashi Y, Bigler D, Chang A, Yamashita Y, Kincade PW, Herr JC, White JM (1999) Role of the integrin-associated protein CD9 in binding between sperm ADAM 2 and the egg integrin alpha6beta1: implications for murine fertilization. Proc Natl Acad Sci U S A 96(21):11830–11835
12. Ovalle S, Gutierrez-Lopez MD, Olmo N, Turnay J, Lizarbe MA, Majano P, Molina-Jimenez F, Lopez-Cabrera M, Yanez-Mo M, Sanchez-Madrid F, Cabanas C (2007) The tetraspanin CD9 inhibits the proliferation and tumorigenicity of human colon carcinoma cells. Int J Cancer 121(10):2140–2152
13. Yanez-Mo M, Barreiro O, Gordon-Alonso M, Sala-Valdes M, Sanchez-Madrid F (2009) Tetraspanin-enriched microdomains: a functional unit in cell plasma membranes. Trends Cell Biol 19(9):434–446
14. Hemler ME (2003) Tetraspanin proteins mediate cellular penetration, invasion, and fusion events and define a novel type of membrane microdomain. Annu Rev Cell Dev Biol 19:397–422
15. Barreiro O, Zamai M, Yanez-Mo M, Tejera E, Lopez-Romero P, Monk PN, Gratton E, Caiolfa VR, Sanchez-Madrid F (2008) Endothelial adhesion receptors are recruited to adherent leukocytes by inclusion in preformed tetraspanin nanoplatforms. J Cell Biol 183(3):527–542
16. Berditchevski F (2001) Complexes of tetraspanins with integrins: more than meets the eye. J Cell Sci 114(Pt 23):4143–4151
17. Yan Y, Shirakabe K, Werb Z (2002) The metalloprotease Kuzbanian (ADAM10) mediates the transactivation of EGF receptor by G protein-coupled receptors. J Cell Biol 158(2):221–226
18. Takahashi Y, Bigler D, Ito Y, White JM (2001) Sequence-specific interaction between the disintegrin domain of mouse ADAM 3 and murine eggs: role of beta1 integrin-associated proteins CD9, CD81, and CD98. Mol Biol Cell 12(4):809–820
19. Arduise C, Abache T, Li L, Billard M, Chabanon A, Ludwig A, Mauduit P, Boucheix C, Rubinstein E, Le Naour F (2008) Tetraspanins regulate ADAM10-mediated cleavage of TNF-alpha and epidermal growth factor. J Immunol 181(10):7002–7013
20. Barreiro O, Yanez-Mo M, Sala-Valdes M, Gutierrez-Lopez MD, Ovalle S, Higginbottom A, Monk PN, Cabanas C, Sanchez-Madrid F (2005) Endothelial tetraspanin microdomains regulate leukocyte firm adhesion during extravasation. Blood 105(7):2852–2861
21. Gonzalez-Alvaro I, Dominguez-Jimenez C, Ortiz AM, Nunez-Gonzalez V, Roda-Navarro P, Fernandez-Ruiz E, Sancho D, Sanchez-Madrid F (2006) Interleukin-15 and interferon-gamma participate in the cross-talk between natural killer and monocytic cells required for tumour necrosis factor production. Arthritis Res Ther 8(4):R88
22. Gutierrez-Lopez MD, Ovalle S, Yanez-Mo M, Sanchez-Sanchez N, Rubinstein E, Olmo N, Lizarbe MA, Sanchez-Madrid F, Cabanas C (2003) A functionally relevant conformational epitope on the CD9 tetraspanin depends on the association with activated beta1 integrin. J Biol Chem 278(1):208–218
23. Arroyo AG, Sanchez-Mateos P, Campanero MR, Martin-Padura I, Dejana E, Sanchez-Madrid F (1992) Regulation of the VLA integrin-ligand interactions through the beta 1 subunit. J Cell Biol 117(3):659–670

24. Yanez-Mo M, Alfranca A, Cabanas C, Marazuela M, Tejedor R, Ursa MA, Ashman LK, de Landazuri MO, Sanchez-Madrid F (1998) Regulation of endothelial cell motility by complexes of tetraspan molecules CD81/TAPA-1 and CD151/PETA-3 with alpha3 beta1 integrin localized at endothelial lateral junctions. J Cell Biol 141(3):791–804
25. Higginbottom A, Takahashi Y, Bolling L, Coonrod SA, White JM, Partridge LJ, Monk PN (2003) Structural requirements for the inhibitory action of the CD9 large extracellular domain in sperm/oocyte binding and fusion. Biochem Biophys Res Commun 311(1):208–214
26. Bax DV, Messent AJ, Tart J, van Hoang M, Kott J, Maciewicz RA, Humphries MJ (2004) Integrin alpha5beta1 and ADAM-17 interact in vitro and co-localize in migrating HeLa cells. J Biol Chem 279(21):22377–22386
27. Isler P, Vey E, Zhang JH, Dayer JM (1993) Cell surface glycoproteins expressed on activated human T cells induce production of interleukin-1 beta by monocytic cells: a possible role of CD69. Eur Cytokine Netw 4(1):15–23
28. Kovalenko OV, Yang X, Kolesnikova TV, Hemler ME (2004) Evidence for specific tetraspanin homodimers: inhibition of palmitoylation makes cysteine residues available for cross-linking. Biochem J 377(Pt 2):407–417
29. Le Naour F, Andre M, Boucheix C, Rubinstein E (2006) Membrane microdomains and proteomics: lessons from tetraspanin microdomains and comparison with lipid rafts. Proteomics 6(24):6447–6454
30. Ouchi N, Kihara S, Yamashita S, Higashiyama S, Nakagawa T, Shimomura I, Funahashi T, Kameda-Takemura K, Kawata S, Taniguchi N, Matsuzawa Y (1997) Role of membrane-anchored heparin-binding epidermal growth factor-like growth factor and CD9 on macrophages. Biochem J 328(Pt 3):923–928
31. Doedens JR, Mahimkar RM, Black RA (2003) TACE/ADAM-17 enzymatic activity is increased in response to cellular stimulation. Biochem Biophys Res Commun 308(2):331–338
32. Glaser KB, Pease L, Li J, Morgan DW (1999) Enhancement of the surface expression of tumor necrosis factor alpha (TNFalpha) but not the p55 TNFalpha receptor in the THP-1 monocytic cell line by matrix metalloprotease inhibitors. Biochem Pharmacol 57(3):291–302
33. Becker BF, Gilles S, Sommerhoff CP, Zahler S (2002) Application of peptides containing the cleavage sequence of pro-TNFalpha in assessing TACE activity of whole cells. Biol Chem 383(11):1821–1826
34. Rabie T, Strehl A, Ludwig A, Nieswandt B (2005) Evidence for a role of ADAM17 (TACE) in the regulation of platelet glycoprotein V. J Biol Chem 280(15):14462–14468
35. Zhao XJ, Oliver P, Song K, Schurr J, Zhang Z, Kolls JK (2004) Chronic ethanol enhances ectodomain shedding in T cells and monocytes. Alcohol Clin Exp Res 28(9):1399–1407
36. Condon TP, Flournoy S, Sawyer GJ, Baker BF, Kishimoto TK, Bennett CF (2001) ADAM17 but not ADAM10 mediates tumor necrosis factor-alpha and L-selectin shedding from leukocyte membranes. Antisense Nucleic Acid Drug Dev 11(2):107–116
37. Luscinskas FW, Cybulsky MI, Kiely JM, Peckins CS, Davis VM, Gimbrone MA Jr (1991) Cytokine-activated human endothelial monolayers support enhanced neutrophil transmigration via a mechanism involving both endothelial-leukocyte adhesion molecule-1 and intercellular adhesion molecule-1. J Immunol 146(5):1617–1625
38. Montero JC, Yuste L, Diaz-Rodriguez E, Esparis-Ogando A, Pandiella A (2002) Mitogen-activated protein kinase-dependent and -independent routes control shedding of transmembrane growth factors through multiple secretases. Biochem J 363(Pt 2):211–221
39. Reddy P, Slack JL, Davis R, Cerretti DP, Kozlosky CJ, Blanton RA, Shows D, Peschon JJ, Black RA (2000) Functional analysis of the domain structure of tumor necrosis factor-alpha converting enzyme. J Biol Chem 275(19):14608–14614
40. Canault M, Tellier E, Bonardo B, Mas E, Aumailley M, Juhan-Vague I, Nalbone G, Peiretti F (2006) FHL2 interacts with both ADAM-17 and the cytoskeleton and regulates ADAM-17 localization and activity. J Cell Physiol 208(2):363–372
41. Nishi E, Hiraoka Y, Yoshida K, Okawa K, Kita T (2006) Nardilysin enhances ectodomain shedding of heparin-binding epidermal growth factor-like growth factor through activation of tumor necrosis factor-alpha-converting enzyme. J Biol Chem 281(41):31164–31172
42. Zheng Y, Schlondorff J, Blobel CP (2002) Evidence for regulation of the tumor necrosis factor alpha-convertase (TACE) by protein-tyrosine phosphatase PTPH1. J Biol Chem 277(45): 42463–42470
43. Peiretti F, Deprez-Beauclair P, Bonardo B, Aubert H, Juhan-Vague I, Nalbone G (2003) Identification of SAP97 as an intracellular binding partner of TACE. J Cell Sci 116(Pt 10): 1949–1957
44. Ho SH, Martin F, Higginbottom A, Partridge LJ, Parthasarathy V, Moseley GW, Lopez P, Cheng-Mayer C, Monk PN (2006) Recombinant extracellular domains of tetraspanin proteins are potent inhibitors of the infection of macrophages by human immunodeficiency virus type 1. J Virol 80(13):6487–6496
45. Xu D, Sharma C, Hemler ME (2009) Tetraspanin12 regulates ADAM10-dependent cleavage of amyloid precursor protein. Faseb J 23(11):3674–3681
46. Charrin S, le Naour F, Silvie O, Milhiet PE, Boucheix C, Rubinstein E (2009) Lateral organization of membrane proteins: tetraspanins spin their web. Biochem J 420(2):133–154
47. Nishiuchi R, Sanzen N, Nada S, Sumida Y, Wada Y, Okada M, Takagi J, Hasegawa H, Sekiguchi K (2005) Potentiation of the ligand-binding activity of integrin alpha3beta1 via association with tetraspanin CD151. Proc Natl Acad Sci U S A 102(6): 1939–1944
48. Shi W, Fan H, Shum L, Derynck R (2000) The tetraspanin CD9 associates with transmembrane TGF-alpha and regulates TGF-alpha-induced EGF receptor activation and cell proliferation. J Cell Biol 148(3):591–602
49. Reiss K, Saftig P (2009) The "a disintegrin and metalloprotease" (ADAM) family of sheddases: physiological and cellular functions. Semin Cell Dev Biol 20(2):126–137
50. Ludwig A, Hundhausen C, Lambert MH, Broadway N, Andrews RC, Bickett DM, Leesnitzer MA, Becherer JD (2005) Metalloproteinase inhibitors for the disintegrin-like metalloproteinases ADAM10 and ADAM17 that differentially block constitutive and phorbol ester-inducible shedding of cell surface molecules. Comb Chem High Throughput Screen 8(2):161–171
51. Yanez-Mo M, Barreiro O, Gonzalo P, Batista A, Megias D, Genis L, Sachs N, Sala-Valdes M, Alonso MA, Montoya MC, Sonnenberg A, Arroyo AG, Sanchez-Madrid F (2008) MT1-MMP collagenolytic activity is regulated through association with tetraspanin CD151 in primary endothelial cells. Blood 112(8): 3217–3226
52. Lafleur MA, Xu D, Hemler ME (2009) Tetraspanin proteins regulate membrane type-1 matrix metalloproteinase-dependent pericellular proteolysis. Mol Biol Cell 20(7):2030–2040